EUR 2963.e

EUROPEAN ATOMIC ENERGY COMMUNITY - EURATOM
FIAT S.p.A., Sezione Energia Nucleare - Torino
Società ANSALDO S.p.A. - Genova

FORCED CONVECTION BURNOUT AND HYDRODYNAMIC INSTABILITY EXPERIMENTS FOR WATER AT HIGH PRESSURE

Part II : Presentation of Data for Water Flowing Upward Along a Uniformly Heated Rod in a Square Unheated Duct

by

A. CAMPANILE, G. GALIMI and M. GOFFI
(SORIN, Centro Ricerche Nucleari, Saluggia, Italia)

1966

Contract No. 008-61-12 PNII

This report is on sale at the addresses listed on cover page 4

at the price of FF 5,—	FB 50,—	DM 4,—	Lit. 620	Fl. 3,60

When ordening, please quote the EUR number and the title, which are indicated on the cover of each report.

Printed by Guyot, s.a.
Brussels, August 1966

EUR 2963.e

FORCED CONVECTION BURNOUT AND HYDRODYNAMIC INSTABILITY EXPERIMENTS FOR WATER AT HIGH PRESSURE - PART II: PRESENTATION OF DATA FOR WATER FLOWING UPWARD ALONG A UNIFORMLY HEATED ROD IN A SQUARE UNHEATED DUCT
by. A. CAMPANILE, G. GALIMI and M. GOFFI (SORIN, Centro Ricerche Nucleari, Saluggia, Italia)

European Atomic Energy Community - EURATOM
FIAT S.p.A., Sezione Energia Nucleare - Torino (Italia)
Società ANSALDO S.p.A. - Genova (Italia)
Contract No. 008-61-12 PNII
Brussels, August 1966 - 28 Pages - 17 Figures - FB 50

N. 110 burnout data for water flowing upward, in conditions of forced convection at high pressure, in a vertical square annular channel were taken over a wide range of mass flow rate, inlet subcooling and pressure.

EUR 2963.e

FORCED CONVECTION BURNOUT AND HYDRODYNAMIC INSTABILITY EXPERIMENTS FOR WATER AT HIGH PRESSURE - PART II: PRESENTATION OF DATA FOR WATER FLOWING UPWARD ALONG A UNIFORMLY HEATED ROD IN A SQUARE UNHEATED DUCT
by. A. CAMPANILE, G. GALIMI and M. GOFFI (SORIN, Centro Ricerche Nucleari, Saluggia, Italia)

European Atomic Energy Community - EURATOM
FIAT S.p.A., Sezione Energia Nucleare - Torino (Italia)
Società ANSALDO S.p.A. - Genova (Italia)
Contract No. 008-61-12 PNII
Brussels, August 1966 - 28 Pages - 17 Figures - FB 50

N. 110 burnout data for water flowing upward, in conditions of forced convection at high pressure, in a vertical square annular channel were taken over a wide range of mass flow rate, inlet subcooling and pressure.

EUR 2963.e

FORCED CONVECTION BURNOUT AND HYDRODYNAMIC INSTABILITY EXPERIMENTS FOR WATER AT HIGH PRESSURE - PART II: PRESENTATION OF DATA FOR WATER FLOWING UPWARD ALONG A UNIFORMLY HEATED ROD IN A SQUARE UNHEATED DUCT
by. A. CAMPANILE, G. GALIMI and M. GOFFI (SORIN, Centro Ricerche Nucleari, Saluggia, Italia)

European Atomic Energy Community - EURATOM
FIAT S.p.A., Sezione Energia Nucleare - Torino (Italia)
Società ANSALDO S.p.A. - Genova (Italia)
Contract No. 008-61-12 PNII
Brussels, August 1966 - 28 Pages - 17 Figures - FB 50

N. 110 burnout data for water flowing upward, in conditions of forced convection at high pressure, in a vertical square annular channel were taken over a wide range of mass flow rate, inlet subcooling and pressure.

The data refer to a configuration of the cross section geometry in which a heater rod is centered in a square unheated channel. Only two data could be taken with eccentric transverse position of the rod in the flow channel before physical destruction of the heater.

The data refer to a configuration of the cross section geometry in which a heater rod is centered in a square unheated channel. Only two data could be taken with eccentric transverse position of the rod in the flow channel before physical destruction of the heater.

The data refer to a configuration of the cross section geometry in which a heater rod is centered in a square unheated channel. Only two data could be taken with eccentric transverse position of the rod in the flow channel before physical destruction of the heater.

EUR 2963.e

EUROPEAN ATOMIC ENERGY COMMUNITY - EURATOM
FIAT S.p.A., Sezione Energia Nucleare - Torino
Società ANSALDO S.p.A. - Genova

FORCED CONVECTION BURNOUT AND HYDRODYNAMIC INSTABILITY EXPERIMENTS FOR WATER AT HIGH PRESSURE

Part II : Presentation of Data for Water Flowing Upward Along a Uniformly Heated Rod in a Square Unheated Duct

by

A. CAMPANILE, G. GALIMI and M. GOFFI
(SORIN, Centro Ricerche Nucleari, Saluggia, Italia)

1966

Contract No. 008-61-12 PNII

CONTENTS

SUMMARY

N. 110 burnout data for water flowing upward, in conditions of forced convection at high pressure, in a vertical square annular channel were taken over a wide range of mass flow rate, inlet subcooling and pressure.

The data refer to a configuration of the cross section geometry in which a heater rod is centered in a square unheated channel. Only two data could be taken with eccentric transverse position of the rod in the flow channel before physical destruction of the heater.

1. Introduction

In water reactor cores, with fuel elements consisting of rod bundles, the majority of the cells of the flow area receive heat almost symmetrically from the contour (cells amid the fuel rods). However the presence of structural elements (fuel assembly cans, control system members) within the core involves the shaping of coolant channels surrounded by either heating rods and unheated walls.

In most cases close clearances exist between fuel rods and unheated walls. In addition, the accidental case of a rod contacting a structural member brings about the problem of assessing to which extent burnout is affected in such instances. Probably in case like this the parameters will affect the DNB in a way different from that of a straight flow channel.

The peculiar condition of heated rod facing an unheated wall might conceivably have some influence on the onset and development of the thermal crisis occurring on the power generating surface, expecially in the case of very narrow gaps and low values of the outlet quality.

In the frame of the forced convection burnout studies carried out at SORIN Research Center as support to the EURATOM - FIAT - ANSALDO contract for nuclear ship propulsion design study, a research program has been undertaken for the particular purpose of investigating the effect, if any, on burnout due to a possible interaction between heated and unheated walls.

The attention has been focused on the situation of a corner

Manuscript received on May 25, 1966.

rod in a fuel assembly can, having two sides surrounded by structural walls.

For a better simulation, the square annular geometry has been pref erred to the circular annulus, with provision for moving the heater rod along the diagonal of the square can in order to set the rod at positions closer and closer to both unheated side walls.

The entire experimental program on this subject should include the following sets of tests:

a) D N B tests with heater rods of different lengths and diameters positioned in the center of the square cans of different flow area.

b) D N B tests with heater rod off-centered in the square can.

c) D N B tests with heater rod in corner position in contact with unheated walls.

The experiments described in this report deal with measurement of burnout heat fluxes on square annular channel consisting of 10.2 mm O.D. heater rod centered in a 15 x 15 mm unheated square channel, cooled by water at high pressure flowing upward.

Tests have been made with two lenghts of the heater in wide ranges of specific mass flow rate, quality and pressure.

Tests were performed at the SORIN heat transfer Lab. in Saluggia, making use of the 600 KW high pressure water loop described in detail in the EUR Report 2490.e.

What was there specified with regard to instrumentation, measurement precisions, test procedures and burnourt definition, applies also to the experiments here reported. Only the test section expressly made for these experiments, will be described in detail.

2. Description of the test section

The test section is basically an unheated rectangular flow channel enclosing a heater rod, that may be either centered in the channel or set at different positions along the diagonal of the square flow area. Fig. 1 and 2 show an exploded and assembled view of the test section respectively.

Both flow channel and heater rod are inserted in a test section housing designed to withstand the pressure.

The housing was made of 304 stainless-steel 2" schedule 80 tube and fittings, to which were welded two 1" tubes as flow connections and a side flanged extension for the lower electrical power connection to the heater. This consist of a nickel leaf spring designed to allow axial expasion of the heater rod. Fig. 3 is an assembly drawing of the test section and Fig. 4 shows the assembled channel being inserted in the pressure housing.

Both ends of the container are flanged, the upper flange being connected to the upper electrical power connection and the lower one being provided to allow fastening of the heater rod to the lower power connection after insertion into the pressure housing.

The flanges welded to the electrodes are electrically insulated from the mating flanges by means of compressed asbestos gaskets.

The heater was made of 316 stainless steel tubing 10.2 mm O.D. by 6.2 mm I.D. Two Values of the heated portion length were tested, 560 mm and 1183 mm respectively.

Nickel extension were welded at each end of the heater rod for connection to the power terminals. The heated lenght of the heater was internally fitted with four steel wires welded to the wall of the tube and mutually insulated by multiholes aluminum oxide ceramics.

These wires provided voltage taps for voltage drop measure ment and for resistance bridge burnout detection. Voltage taps were respectively located at the outlet end, 100 mm below this point, at the middle point and at the inlet end of the heated portion of the heater rod.

The rod was spring loaded to prevent it from buckling during burnout experiments.

The outlet nickel extension of the heater was welded to the upper electrode, the lower one being connected, after insertion into the housing, to the nickel leaf spring electrode by means of a bolted connection.

The square duct is composed of two halves of a stainless rod milled on their maiting faces to produce a square flow passage.

Coupling of the two channel halves is accomplished through 10 pairs of positioning pins and 15 pairs of fastening screws.

The square channel presents two cilindrical ends that allow its positioning in the test section housing. Special replaceable terminal rings provide the possibility of changing the transverse position of the heater element in the flow channel from a centered position to a corner one closer to the unheated walls.

In addition, the square duct is equipped at different heights with sets of 4 adjustable ceramic pins for fine adjustament of the transverse position of the heater and to prevent this from coming in contact with the duct walls wich are at ground potential.

Spy-holes, equipped with plugs, provide a means of checking clearances between heater and duct walls by means of a precision dial gauge. In the centered assembly, the sets of spacers closest to the outlet were at 350 mm below and 20 mm beyond the outlet end of the heated portion of the rod.

In the asymmetric assembly the corresponding distances were 146 mm and 20 mm respectively.

Water temperature was measured with thermocouples of the stainless steel sheath type. Two such thermocouples were located at the inlet end of the heated section of the rod for water inlet temperature measurement. As for the outlet, two thermocouples were used for the centered and asymmetric assembly as shown in Fig. 5.

This figure indicate also the relevant dimensions of the flow area of the channel.

The duct was also equipped with pressure taps at the inlet and outlet for pressure drop measurement. The test section is mounted vertically in the loop with subcooled water entering at the bottom.

3. Experimental burnout data

3.1. Parameter ranges

The experiments were carried out under different physical conditions within the following parameter ranges:

Pressure	from	33	ata	to	134	ata
Mass flow rate	"	69		"	419	gr/cm^2 sec
Inlet suheading	"	1		"	160	°C

The range of dependent variables were experimentally found as follows:

Average burnout heat flux:	from	104	to	709	$\frac{watt}{cm^2}$
Exit quality :	"	-49%	"	+21%	

3.2. Data tabulation

The experimental burn-out results obtained on the single heated rod fitted in the square duct are given in Tables I through VI.

Total burnout power as well as average burnout heat fluxes are reported. Computation of the average values of the heat flux is based on the assumption of power being uniformly distributed over the external surface of the heater.

Average values of the heat flux based on the measurement of the voltage drop over the top 10 cm length of the heater, have been also tabulated whenever this measurement was taken.

Tabulated values of power density are referred to the volume of coolant contained within the flow channel.

For almost all tests two values of the coolant temperature, taken in corrispondence of two different positions of the exit flow area, have been reported.

Fig. 5 shows the location of the thermocouple hot junctions employed for these measurements. The Tables report also the values of the exit water temperature resulting from heat balance calculations.

Reported values of the pressure drop are based on measurements taken across two pressure taps located on the square duct, in corrispondence of the ends of the heated portion of the rod. These values account also for the elevation pressure drop.

In Table VI two burnout data are quoted referring to the asymmetric setting of the heater in the square duct. As previously said, only these two points could be obtained from this test section because of the occurence of a physical burnout.

3.3. Graphical representations

Burn-out data, obtained with the centered configuration of the heater have been plotted in Fig. 6 through 17.

Burnout power as function of inlet subcooling for the two heater lengths tested, are graphically shown in Fig. 6 through 9.

Holding the mass flow rate constant, the effect of pressure have been made evident in Fig. 10 through 13, where burnout power is plotted versus inlet temperature. The representation refers to both heater lengths tested allowing comparison of channels of different length and same inlet conditions.

In Fig. 14 through 17 average values of burnout heat fluxes at 132 ata have been plotted versus outlet steam quality showing the influence of the heated length for equal outlet conditions.

4. Remarks on the experimental results

The data here reported refer to a channel in which only a part of the wetted perimeter is heated. Hence in such a geometrical arrangement the equivalent diameter, defined as:

$$D_e = 4 \times \frac{\text{Total flow area}}{\text{Total wetted perimeter}} = 6.23 \text{ mm}$$

is lower than the diameter D_n defined as:

$$D_n = 4 \times \frac{\text{Total flow area}}{\text{Heated perimeter}} = 17.89 \text{ mm}$$

The dependence of the burnout upon the heat flux as well as local thermal conditions of the coolant, would suggest, at first glance, the adequacy of the parameter D_n, in addition to the length of the heater, to represent the geometry of channels of any shapes.

This simple assumption is based on the consideration that, for equal mass flow rate and fluid inlet conditions, channels having the same D_n would exhibit the same average outlet enthalpy if they had equal heat fluxes.

A comparison of the present data with burnout results obtained in round tubes having comparable values of heated length and D_n, has shown that the above mentioned criterion of similarity based on D_n concept seems adequate in most cases. This appeared evident for high pressure tests (132 ata) with the exception for those performed at lower inlet subcooling for which the burnout power measured in the square duct was somewhat higher than corresponding values for tubes.

At lower pressure (84 ata), it has been noted that the similarity doesn't old in all cases, inasmuch as with decreasing the mass flow rate, the burnout power for the square annulus appeard to be always lower than the corresponding treshold for tubes of comparable D_n and length.

Examination of the reported values of the exit water temperature shows the existence of a generally rilevant transversal drop of temperature going from the heated to the unheated surface.

The difference between the two measured values of temperature increases with increasing heat fluxes and depends also upon mass flow rate and exit quality.

The last two parameters tend both to flatten, with their increase, the water temperature distribution across the flow area.

The study of the liquid temperature field seems very interesting to the purpose of evaluating the actual steam quality when thermodynamic equilibrium has not been attained and of providing information about the flow distribution in the channel area induced by the presence of the unheated wall.

For instance, examination of the exit water temperatures measured during the tests with the rod off-center, shows that thermocouples placed at the same distance from the rod, measure a higher water enthalpy rise in the narrower gap, so indicating a non uniform distribution of the flow around the rod.

By comparing equivalent data obtained with channels having the rod in the center or out of it, it might be inferred that gaps smaller than 90 mils have lower burnout power treshold. Obviously such a conclusion cannot be drawn, on the basis of two experiments only, and additional work is required in this area to evaluate the role played by the distance in the interaction between heated and unheated wall.

Acknowledgements

The authors wish to express their appreciation to Mr. O. Morocutti of EURATOM as well as to Messrs. G. Previti and P. Grillo, both of FIAT Sezione Energia Nucleare, for their constant co-operation and support.

The valuable assistance and essential contributions of Mr. G. Fumero, P. Minazio and G. Passavanti of the SORIN heat transfer Lab. throughout the design, testing and data elaboration works is deeply appreciated.

Finally, the authors are grateful to the SORIN computing staff for data processing and computer programming and to the SORIN general workshop for the fabrication of the test section.

The contribution of Mr. F. Biancone, in charge of the design of experimental facilities up to 1966, is deeply appreciated.

TABLE I

Burnout data for centered heater 560 mm long. Nominal pressure: 34 - 84 ata.

Run	Pressure ata	Flow l/h	Mass flow rate gr/cm^2 sec	Inlet subcooling °C	Inlet temperature °C	Exit temperature °C: Actual values b: 4.5 mm	Exit temperature °C: Actual values a: 1.4 mm	Exit temperature °C: Thermal balance value	Power kW	Average heat flux $watt/cm^2$	Exit average heat flux $watt/cm^2$	Power density $watt/cm^3$	Pressure drop gr/cm^2	Exit quality %
60 (11-6-65)	33.5	570	92,2	10.6	227.9	239	239	239	40.9	228,0	223	510.3	—	13.5
51 (11-6-65)	33.5	950	153,6	9.8	228.7	239	239	239	55.6	310.0	304.4	693.5	—	11.6
40 (11-6-65)	34	1380	223.0	11.4	224.9	240	240	239.8	69.7	388.6	376.7	868.7	—	8.5
20 (11-6-65)	33.5	2400	387.8	13.6	224.9	239	239	239	84.1	468.9	461.4	1048.4	—	4.9
77 (11-6-65)	33.2	2240	388.6	64.8	173.7	209.5	224.7	217	108.6	605.5	590.1	1353	—	-5.6
98 (10-6-65)	85.2	570	92.4	71.5	226.6	277.4	288.5	298	56.7	315.4	309.1	707	79	4.9
79 (10-6-65)	83.7	950	153,8	68.9	227.9	270	292.8	291.2	69.2	385.0	374	862.3	105	-2.2
56 (10-6-65)	83.7	1380	224,1	71.5	225.3	265.4	281.7	275.7	78.3	435.6	426.2	976.3	145	-7.9
25 (10-6-65)	83.7	2430	395.6	73.7	223.1	249.8	267.9	260.2	99.7	554.7	541.7	1242.3	275	-13.4

TABLE II

Burnout data for centered heater 560 mm long. Nominal pressure: 126.5 ata.

Run	Pressure ata	Flow l/h	Mass flow rate gr/cm^2 sec	Inlet subcooling °C	Inlet temperature °C	Exit temperature °C: Actual values b: 4 mm	Exit temperature °C: Actual values a: 0.9 mm	Exit temperature °C: Thermal balance value	Power kW	Average heat flux watt/cm^2	Exit average heat flux watt/cm^2	Power density watt/cm^3	Pressure drop gr/cm^2	Exit quality %
15 (10-9-64)	126.2	460	68.5	52	275	295	309	324.4	28	155.8	—	348.9	62	-1.1
68 (15-9-64)	126.2	1050	154.1	46.5	280.5	293	—	317.5	46.5	258.7	255	579.5	52	-5.1
83 (15-9-64)	126.2	1050	154.1	46.5	280.5	295	—	318.2	47	261.5	258	585.7	51	-4.9
13 (16-9-64)	126.2	1100	163.1	50.5	276.5	300	—	313.6	47.5	264.3	—	592	141	-7.4
54 (20-5-64)	125.1	1010	159.6	79.9	246.4	286.6	311.4	295.3	56	311.6	307	697.9	106	-16
50 (16-9-64)	126.2	975	155.8	86.4	240.6	265.2	—	289.5	55	306	—	685.4	125	-18.7
65 (16-9-64)	126.2	975	157.4	93	234	283	—	284.1	55.5	308.8	—	691.7	121	-21.3
36 (29-7-64)	126.2	900	156.6	150	177	207.1	253	246.0	71	395	—	884.8	100	-37.1
28 (16-9-64)	126.2	1850	271.5	46.5	280.5	293	—	304.7	50.5	281	277	629.4	262	-12
35 (21-5-64)	125.1	1760	273.6	70.7	255.6	284	304.9	286.8	63	350.5	—	785.1	200	-19.4
47 (16-9-64)	126.2	1700	271.4	86	241	256	—	276.5	68.5	381.1	376	853.7	210	-24.5
103 (30-7-64)	126.2	1600	271.9	130	197	222.5	265	254.3	106	589.7	—	1321	198	-33.4
80 (29-7-64)	126.2	1565	271.1	145.7	181.3	204	244	234.3	93	517.4	—	1159	166	-42.1
100 (29-7-64)	126.2	2350	405.6	142.5	184.5	203.7	235.1	227.8	113.5	631.5	—	1414.5	309	-44.7

TABLE III

Burnout data for centered heater 560 mm long. Nominal pressure: 132 ata.

Run	Pressure ata	Flow l/h	Mass flow rate gr/cm²sec	Inlet subcooling °C	Inlet temperature °C	Exit temperature °C: Actual values b: 4.5 mm	Exit temperature °C: Actual values a: 1.4 mm	Exit temperature °C: Thermal balance value	Power kW	Average heat flux watt/cm²	Exit average heat flux watt/cm²	Power density watt/cm³	Pressure drop gr/cm²	Exit quality %
125 (1-6-65)	134	750	94.0	3.3	328.3	329.9	—	331.6	26.6	148.0	—	331.5	67	15.5
107 (1-6-65)	131.3	720	91.9	5.7	324.4	329	329.2	330.1	27.7	154.1	151.1	345.1	72	15.1
167 (3-6-65)	134.5	700	97.1	30	302.3	320.8	329.5	331.9	35.6	198.0	195.8	443.8	62	6.1
30 (25-5-65)	131.7	650	90.7	30.3	300	320.4	327.5	329.7	37	205.8	—	461.1	66	8.5
101 (3-6-65)	133.4	630	94.3	57.8	273.5	304.7	314.3	329.4	43.3	240.9	237.3	539.6	53	-1.2
79 (1-6-65)	131.3	605	93.9	72.9	257.2	293.3	297.6	319.4	44.8	249.2	—	558.2	59	-6.4
50 (4-6-65)	128.7	550	88.7	93.9	234.6	278.9	288.7	311.8	50	278.2	274.7	623.1	56	-9.5
42 (8-6-65)	131.3	550	93.4	132.2	197.9	258.4	271	288.9	57.7	321.0	317.8	719	63	-21.8
87 (7-6-65)	131.4	530	92.9	159.5	170.6	243.4	259.5	270.6	60.8	339.0	332.5	758.3	88	-30.1
15 (1-6-65)	132.3	1250	156.1	1.9	328.7	330.6	330.6	330.6	26.2	145.7	145.2	326.4	117	9.2
100 (1-6-65)	133	1190	151.3	5.6	325.4	329.4	329.9	331.1	30.4	169.1	—	378.8	97	9.0
142 (3-6-65)	133.4	1165	159.1	24.2	307.1	321.5	327.6	331.3	38.4	213.6	211.7	478.5	89	1.2
82 (26-5-65)	131.3	1070	148.3	28	302.1	316.8	326.3	330.1	42.4	235.9	232	528.3	99	2.1
44 (26-5-65)	131.3	1070	156.9	48.9	281.2	297.6	312.4	319.1	47.6	264.8	262.2	593.1	91	-6.6
61 (3-6-65)	130.6	1040	153.7	51.4	278.2	300	309.5	318.1	48.6	270.4	263.8	605.6	89	-6.9
81 (3-6-65)	130.8	1040	154.5	53.5	276.1	297.6	306.6	316.1	48.7	270.9	266.9	606.8	83	-7.9
54 (1-6-65)	129.3	1070	161.3	58.9	270.2	291.6	303.2	311.4	51	283.7	—	635.5	88	-9.9
35 (4-6-65)	126.2	955	155.4	99.1	227.9	262.8	280.5	283.1	59.4	330.5	324.7	740.2	80	-22.0
36 (4-6-65)	131.3	955	155.7	103.5	226.6	252	278.6	282.5	60	333.8	330.6	747.7	81	-24.7
24 (8-6-65)	131.3	915	154.9	129.8	200.3	240.9	276.1	266.2	68	378.3	368.4	847.3	82	-31.8

Follows Table III.

Run	Pressure ata	Flow l/h	Mass flow rate gr/cm2sec	Inlet sub cooling °C	Inlet temperature °C	Exit temperature °C: Actual values b: 4.5 mm	Exit temperature °C: Actual values a: 1.4 mm	Exit temperature °C: Thermal balance value	Power kW	Average heat flux watt/cm2	Exit average heat flux watt/cm2	Power density watt/cm3	Pressure drop gr/cm2	Exit quality %
72 (7-6-65)	130.3	880	153.6	154.7	174.8	222	259.5	247.5	72	400.6	382.2	897.6	114	-39.3
114 (1-6-65)	132.7	1700	213.2	2.9	328	329.4	329.7	330.9	30.4	169.1	—	378.8	152	7.1
91 (1-6-65)	133	1715	221.9	9.5	321.5	327.8	329.9	331.1	34.4	191.4	—	428.6	132	3.9
121 (3-6-65)	133.2	1690	231.2	24.6	306.6	318	326.3	326.8	42	233.7	231	523.4	139	-2.7
94 (26-5-65)	131.7	1560	211.8	35.8	294.5	306.6	317	322.1	50.8	282.6	277.9	633	145	-5.1
39 (3-6-65)	130.6	1500	222.9	53.5	276.1	294	302.8	308.8	55.9	311.0	307.2	696.6	123	-11.8
34 (1-6-65)	130.3	1450	222.5	66.9	262.6	281	293.3	299.7	60.8	338.3	—	757.6	118	-16.2
21 (4-6-65)	131.3	1420	231.1	102	228.1	255.2	275.3	273.2	71.3	396.7	390.3	888.5	113	-28.8
12 (8-6-65)	131.3	1320	224.1	132.2	197.9	233.1	263.3	252.9	81	450.6	440.2	1010	110	-37.5
62 (7-6-65)	131.3	1200	210.4	159.5	170.6	208.2	244.1	235.4	87.1	484.6	474.6	1085.4	144	-44.8
110 (1-6-65)	129.3	3150	394.9	1.1	327.8	328.7	328.3	329.1	33	183.6	—	411.2	197	4.5
119 (26-5-65)	131.7	3060	418.5	23.7	306.6	314.6	321.5	322.2	56.8	316.0	312.2	707.8	324	-5.0
106 (3-6-65)	133.4	3000	410.5	24.7	306.6	315.5	321.5	322.4	54	300.4	309.1	672.9	314	-5.9
107 (26-5-65)	131.3	2780	394.9	36.3	293.8	305.7	313.1	314.2	66	367.2	—	822.4	281	-9.1
23 (3-6-65)	130.6	2680	393.7	49.1	280.5	295.2	303.5	314.6	72.9	405.6	396.2	908.3	246	-13.8
15 (3-6-65)	132.3	2680	392.8	49.2	281.5	292.8	301.9	316.8	77	428.4	417.8	959.7	247	-13.4
21 (31-5-65)	130.3	2600	398.3	66.2	263.3	281	290.4	292.8	84.8	471.8	465.8	1056.7	233	-19.6
12 (4-6-65)	131.3	2460	397.6	96.5	233.6	256	275.6	269.0	96	534.1	527	1196.3	221	-30.7
64 (4-6-65)	128.7	2360	401.9	133	195.5	224.2	248.3	239.0	113	628.7	620	1408.1	198	-41.9
53 (7-6-65)	131.4	2280	298.1	155.7	174.4	398.1	237.6	224.9	127.5	709.4	691.6	1588.8	274	-49.1

TABLE IV

Burnout data for centered heater 1183 mm long. Nominal pressure: 34 - 84 ata.

Run	Pressure ata	Flow l/h	Mass flow rate gr/cm²sec	Inlet subcooling °C	Inlet temperature °C	Exit temperature °C			Power kW	Average heat flux watt/cm²	Power density watt/cm³	Pressure drop gr/cm²	Exit quality %
						Actual values		Thermal balance value					
						b: 4.5 mm	a: 1.4 mm						
59 (30-7-65)	33.7	530	91.9	65.1	174.2	199.3	233.9	239.5	53.8	141.9	317.4	194	6.4
27 (30-7-65)	32.5	2280	395.3	61.4	174.1	226.3	237.6	230.2	143.5	378.5	846.6	777	-1.8
193 (29-7-65)	84.2	600	91.9	37	260.3	297.1	320.1	297.2	51.1	134.7	301.5	119	13.6
152 (29-7-65)	83	575	93.2	69.6	226.6	258.7	294.7	296.2	62.8	165.5	370.5	125	8.5
112 (29-7-65)	84.2	550	92.8	98	199.3	236.5	295.2	297.2	69	181.8	407.1	128	2.9
65 (29-7-65)	84.7	530	92.5	125.8	171.8	225.8	295.2	296.9	79.2	208.7	467.2	123	-0.3
184 (29-7-65)	83.7	1005	154.2	37.3	259.5	268.4	295.5	296.8	68.5	180.5	404.1	182	8.0
144 (29-7-65)	84.2	950	153.1	66.2	231	252.7	296.4	297.2	79.6	209.8	469.6	177	2.1
101 (29-7-65)	83.7	915	154.9	99.6	197.2	233.1	296.9	286.2	95.2	250.9	587.1	181	-3.9
63 (29-7-65)	83.7	890	155.5	125.5	171.3	218.6	294	274.3	106.5	280.7	628.3	175	-8.4
175 (29-7-65)	83.2	1450	222.3	36.4	260	267.9	296	296.4	85.5	225.3	504.4	272	5.4
133 (29-7-65)	84.2	1380	222.1	65.2	232	250	296.9	297.2	106	279.3	625.4	254	0.3
89 (29-7-65)	83.7	1350	227.0	94.8	202	231.5	295.2	278.9	119.3	314.4	703.8	266	-6.7
58 (29-7-65)	83.7	1275	222.5	124.3	172.5	213.3	294.5	265.9	137.1	361.3	808.8	231	-11.4
163 (29-7-65)	83.2	2600	397.1	34.9	261.5	270.7	296.1	296.4	121.1	319.1	713.9	539	2.1
121 (29-7-65)	83.7	2460	394.3	61.9	234.9	248.3	296	285	139.9	368.7	825.4	452	-4.6
73 (29-7-65)	83.7	2370	399.8	97	199.8	220.9	293.5	261.3	164.4	433.3	970.0	420	-13.0
49 (29-7-65)	83.7	2280	397.4	123.4	173.4	198.6	289.4	245.8	186.8	492.3	1102.1	390	-18.3

TABLE V

Burnout data for centered heater 1183 mm long. Nominal pressure: 132 ata.

Run	Pressure ata	Flow l/h	Mass flow rate gr/cm² sec	Inlet subcooling °C	Inlet temperature °C	Exit temperature °C: Actual values b: 4.5 mm	Exit temperature °C: Actual values a: 1.4 mm	Exit temperature °C: Thermal balance value	Power kW	Average heat flux watt/cm²	Power density watt/cm³	Pressure drop gr/cm²	Exit quality %
171 (28-7-65)	132	710	91.8	8.9	321.5	318	329.2	330.5	39.4	103.8	232.4	100	21.1
145 (28-7-65)	133	640	91.9	41.3	289.7	302.5	329	331.1	54.8	144.4	323.3	99	14.8
159 (13-7-65)	131	604	93.6	72.2	257.7	290.6	328	329.9	59.4	156.5	350.4	124	3.5
104 (28-7-65)	130.3	570	92.4	98	231.5	272	326.6	329.5	70.8	186.6	417.7	110	1.0
113 (13-7-65)	131.3	570	92.9	102.6	227.4	276.6	327.8	329.1	71.9	189.5	424.2	121	-0.5
100 (28-7-65)	132.3	570	93.4	107.2	223.5	270.5	326.6	325.9	72.2	190.3	426.0	109	-2.5
76 (28-7-65)	131.3	550	93.3	131.5	198.6	260	324.2	323.8	84.6	222.9	499.1	111	-3.8
36 (29-7-65)	130.3	530	92.7	157.2	172.3	238.9	324.2	320.3	96.2	253.5	567.5	118	-5.5
163 (28-7-65)	131.3	1185	152.0	6.9	323.2	319.2	329.2	330.1	47.5	125.2	280.2	149	15.1
123 (28-7-65)	133	1075	152.5	36.5	294.5	301.9	329.2	331.1	62	163.4	365.8	137	5.3
147 (13-7-65)	131.3	1005	154.0	66.8	263.3	285.2	328.7	322.9	72.1	190.0	425.4	152	-4.3
101 (13-7-65)	131.3	955	155.2	100.6	229.5	271	326.8	308.0	87.8	231.4	518.0	151	-12.4
64 (28-7-65)	131.2	915	155.7	133.9	196.2	243.4	323	298.1	109	287.2	643.1	137	-17.4
13 (29-7-65)	132.3	885	154.7	157.5	173.2	221.1	319.4	280.2	109.8	289.4	647.8	130	-26.1

Follows Table V.

Run	Pressure ata	Flow l/h	Mass flow rate gr/cm^2 sec	Inlet subcooling °C	Inlet temperature °C	Exit temperature °C			Power kW	Average heat flux watt/cm^2	Power density watt/cm^3	Pressure drop gr/cm^2	Exit quality %
						Actual values		Thermal balance value					
						b: 4.5 mm	a: 1.4 mm						
154 (28-7-65)	133	1715	222.6	10.2	320.8	316.7	329.2	331.1	53.4	140.7	315.0	205	8.7
111 (28-7-65)	133.3	1556	219.0	34.2	297.1	299	329.2	331.2	70	184.5	413.0	193	1.1
128 (13-7-65)	131.3	1455	222.7	66.3	263.8	283.3	328.3	316.4	89.3	235.3	526.8	217	-8.3
88 (13-7-65)	130.7	1380	224.7	101.8	227.9	261.3	319.6	295.9	107.6	283.6	634.8	206	-18.2
50 (28-7-65)	130.3	1325	224.4	129.6	199.8	235.2	—	283.4	126.8	334.2	748.1	180	-23.8
186 (28-7-65)	132.3	1277	222.9	155.9	174.8	208.1	316	257.0	119.3	314.4	703.8	151	-36.3
149 (28-7-65)	131.3	3060	395.1	8.3	321.8	316.2	329.2	330.1	63.1	166.3	372.3	420	4.9
108 (28-7-65)	132.3	2780	387.9	30.7	300	300	329	327.0	92.1	242.7	543.4	375	-2.2
124 (13-7-65)	130.3	2600	403.0	71.8	257.7	270.2	314.6	300.7	127.1	334.9	749.8	396	-15.7
92 (28-7-65)	130.3	2460	396.9	94.6	234.9	251	311.4	287.5	146.3	385.5	863.1	308	-21.9
76 (13-7-65)	132.7	2460	397.9	97.8	233.1	255.7	305.2	285.0	144.2	380.0	850.7	321	-24.1
25 (28-7-65)	131.3	2360	399.8	130.5	199.6	221.1	—	251.5	160.6	423.2	947.5	269	-34.4
182 (28-7-65)	131.3	2280	397.9	155.3	174.8	197.9	294.5	244.9	179.8	473.8	1060.7	268	-40.8

TABLE VI

Burnout data for out of centre heater 1183 mm along.

Run	Pressure ata	Flow l/h	Mass flow rate gr/cm^2 sec.	Inlet subcooling °C	Inlet temperature °C	Exit temperature °C			Power KW	Average heat flux watt/cm^2	Power density watt/cm^3	Pressure drop gr/cm^2	Exit quality %
						Actual values		Thermal balance value					
						a: 1,88 mm	b: 1,88 mm						
31 (28-10-65)	132,3	660	94,0	37,1	293,6	328,7	309,7	330,6	41,2	108,7	243,1	129	7,0
49 (28-10-65)	132,6	650	93,3	39,8	290,9	329	309,7	330,8	44,6	117,6	263,1	129	8,1

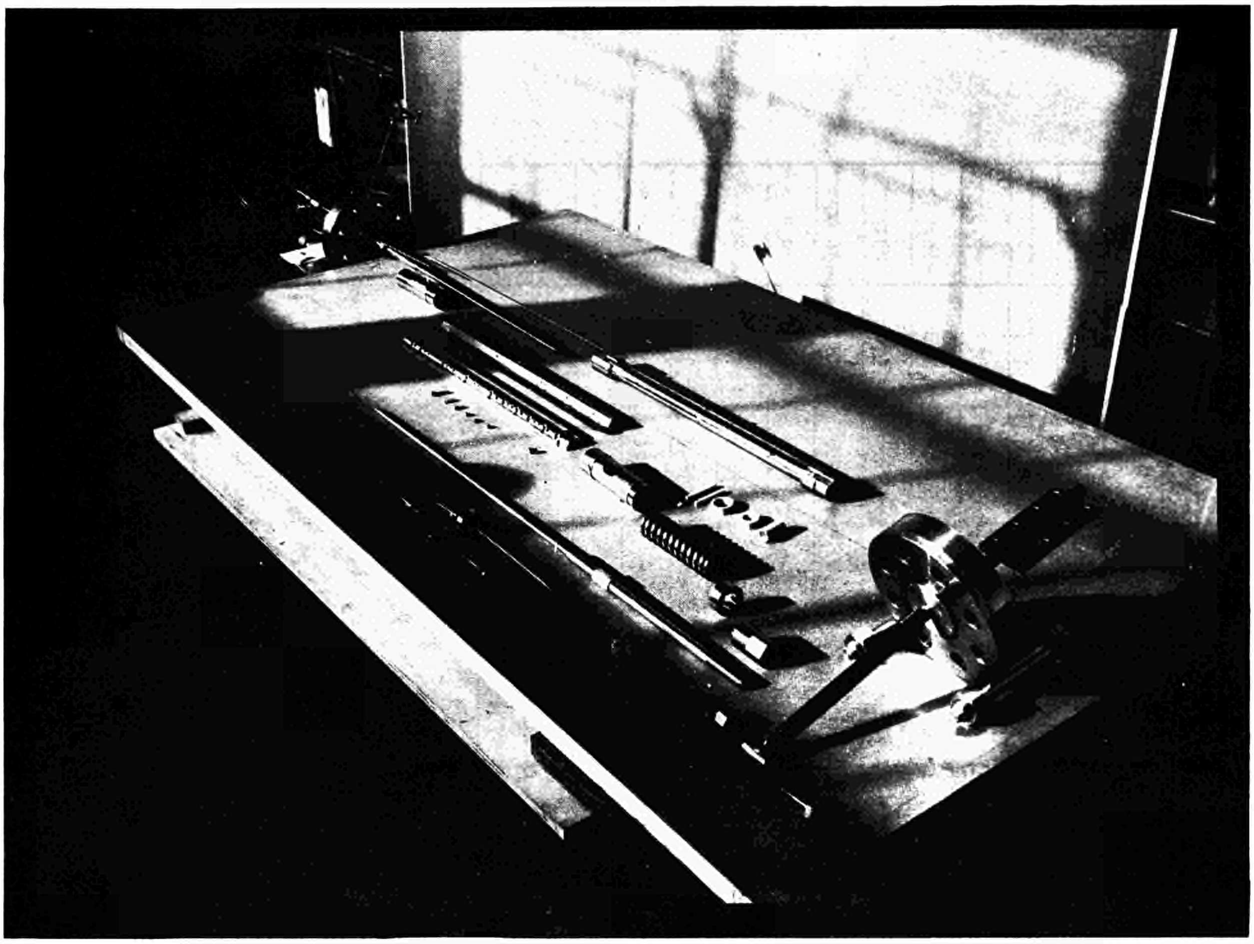

Fig. 1 - Exploded view of the test section.

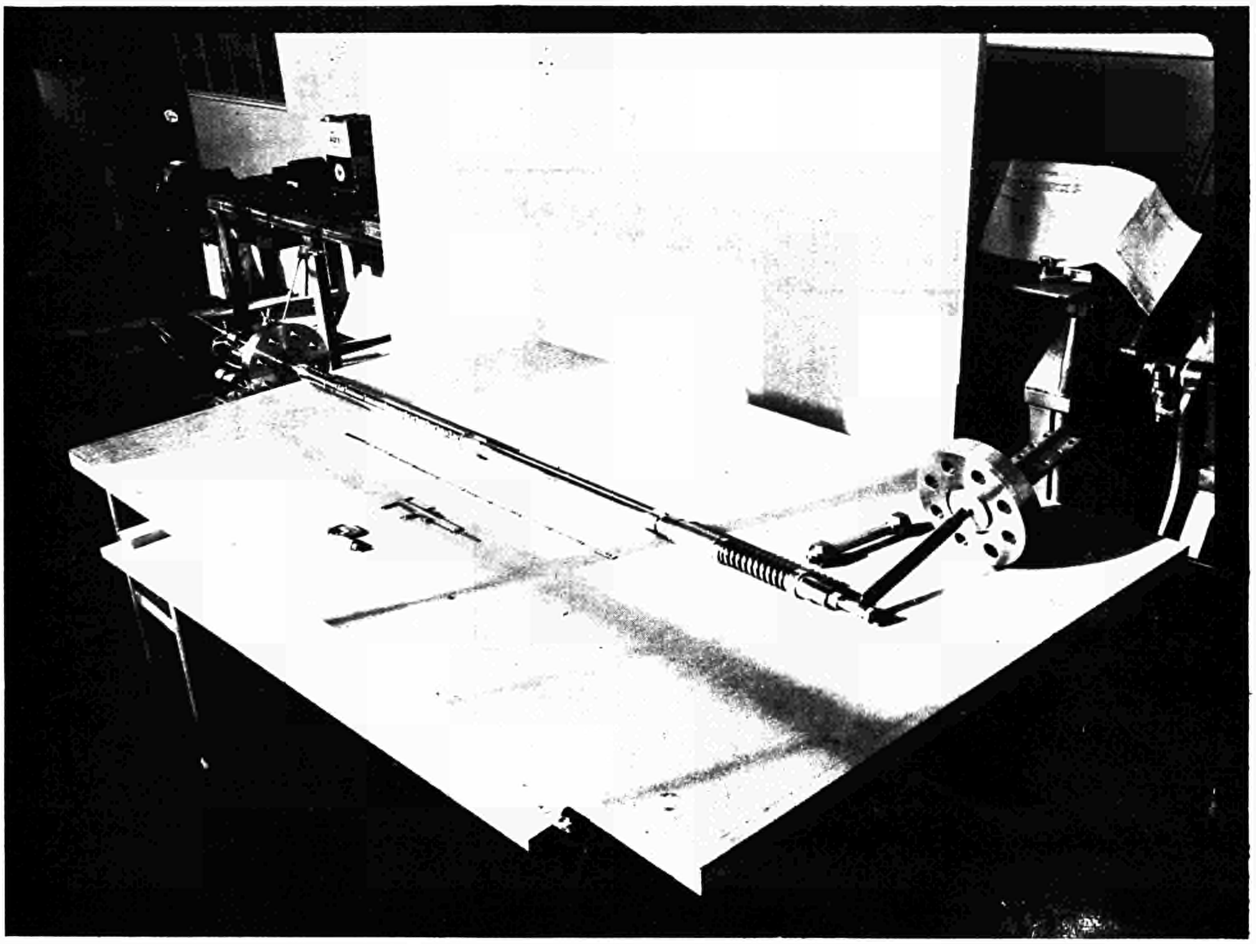

Fig. 2 - Close-up view of the assembled test section.

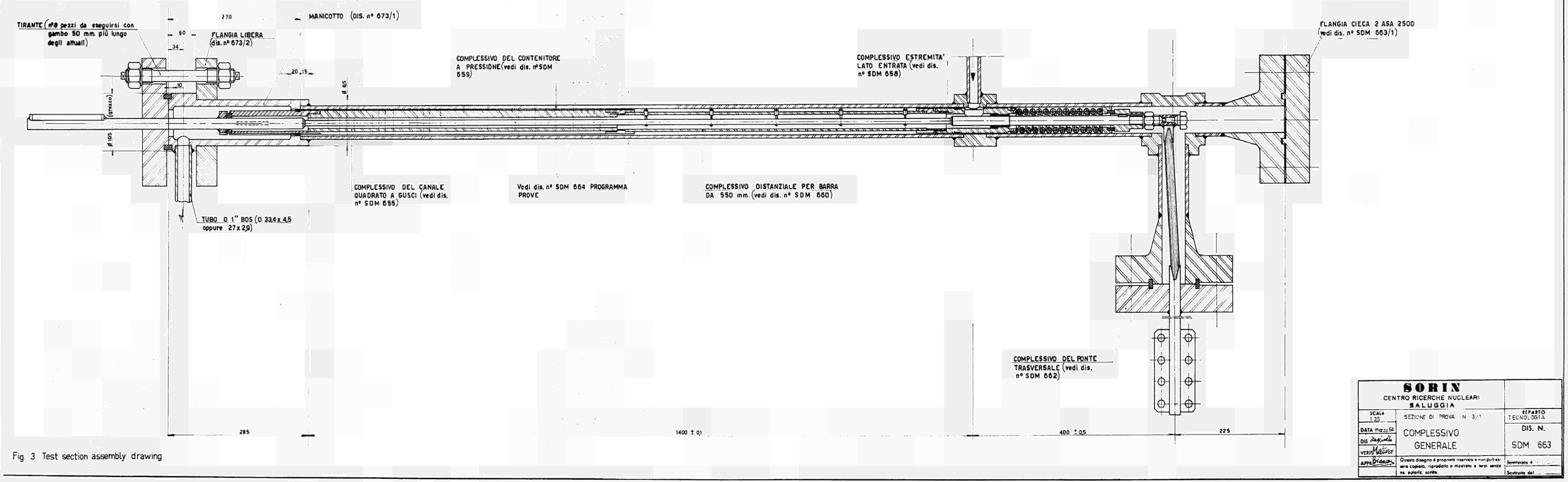

Fig. 3 Test section assembly drawing

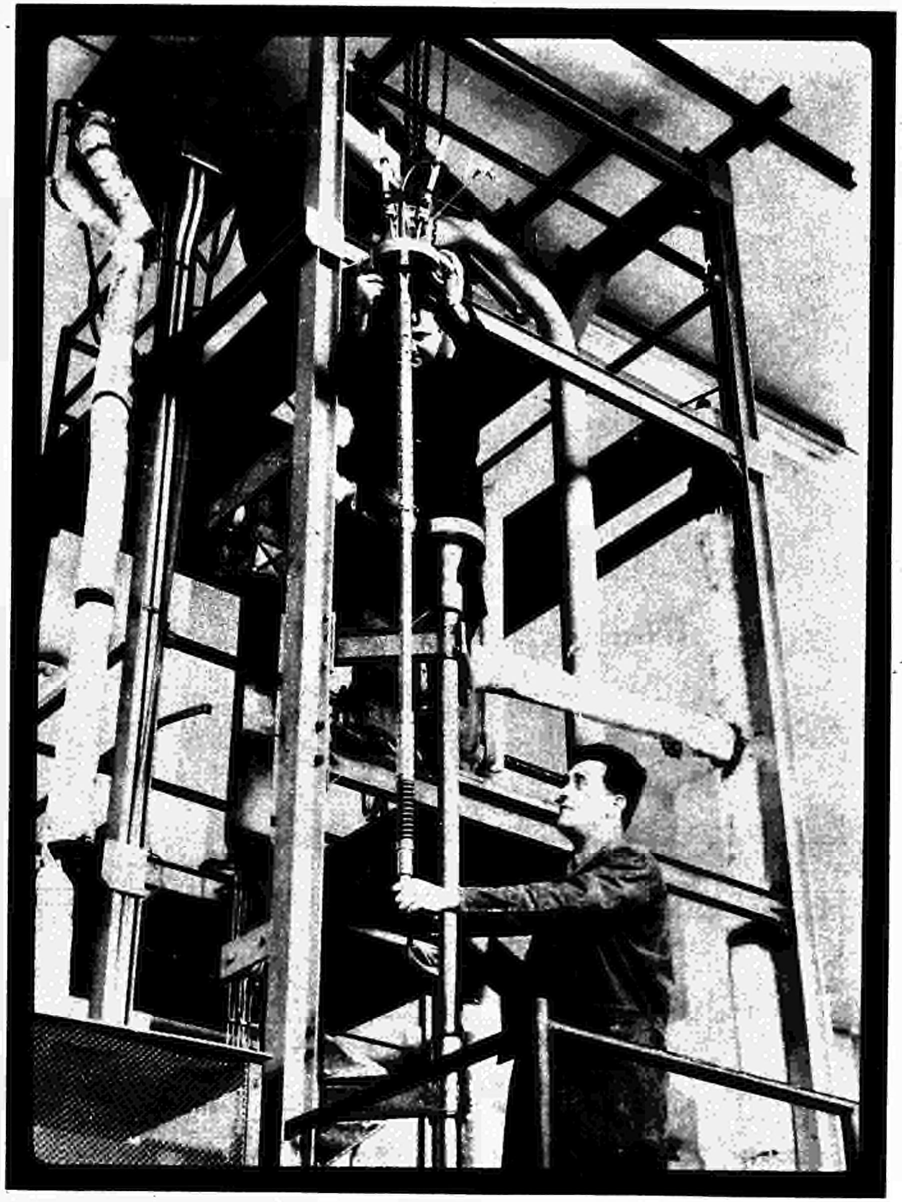

Fig.4 - Test section being inserted in pressure housing.

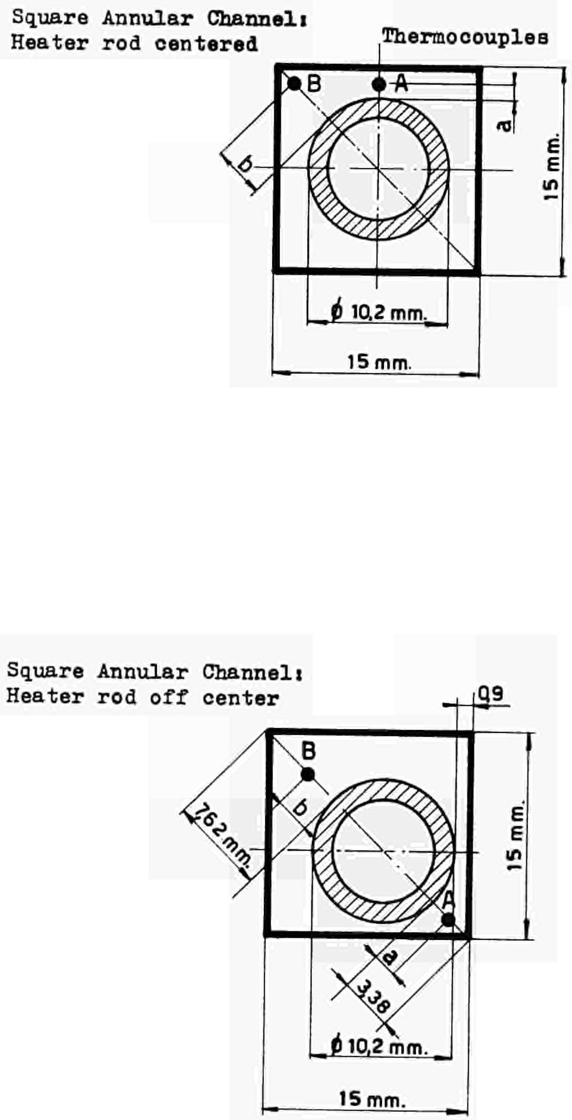

Fig. 5 - Relevant dimensions of the channels showing positions of the exit water temperature probes.

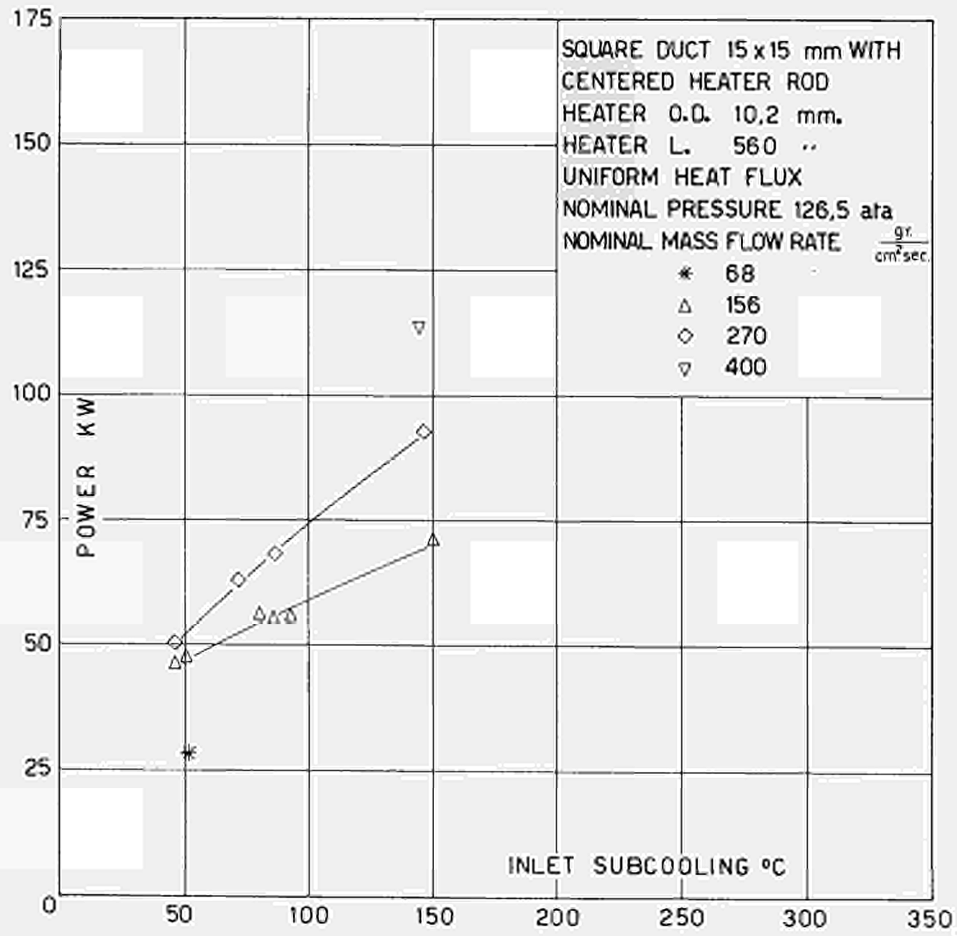

Fig. 6 - Effect of mass flow rate on burnout power. Nominal pressure: 126 ata.

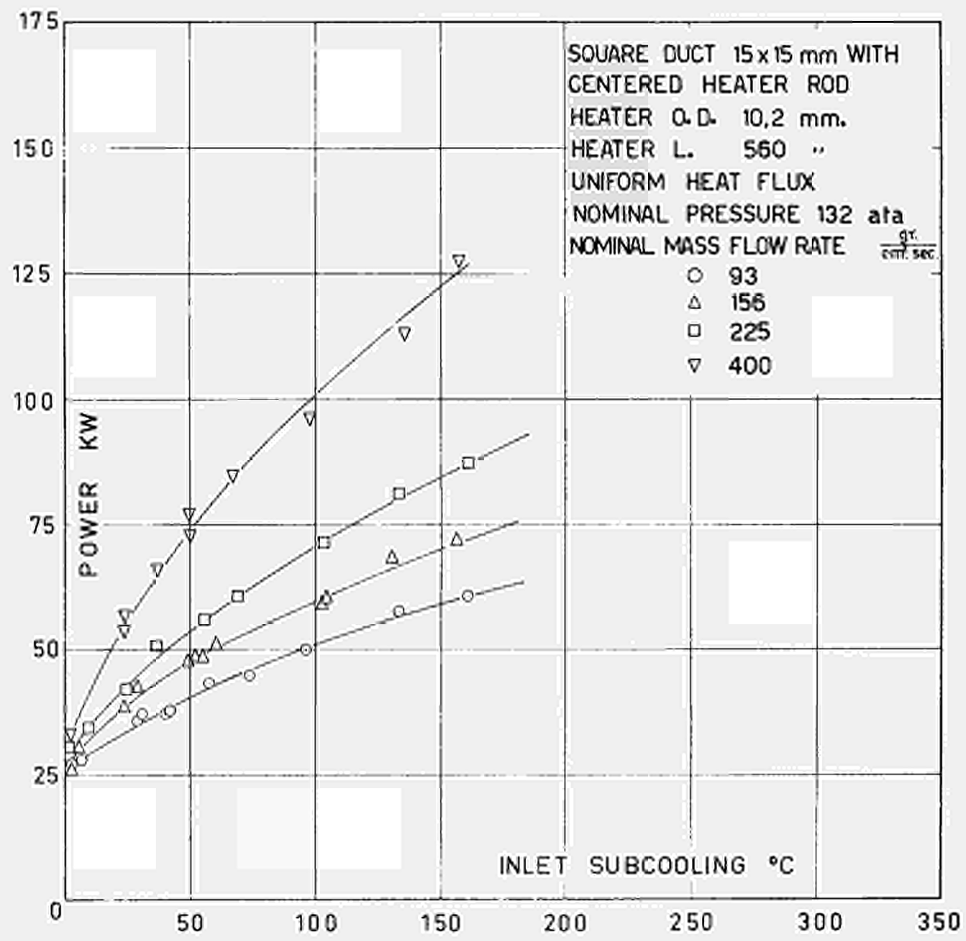

Fig. 7 - Effect of mass flow rate on burnout power. Nominal pressure: 132 ata.

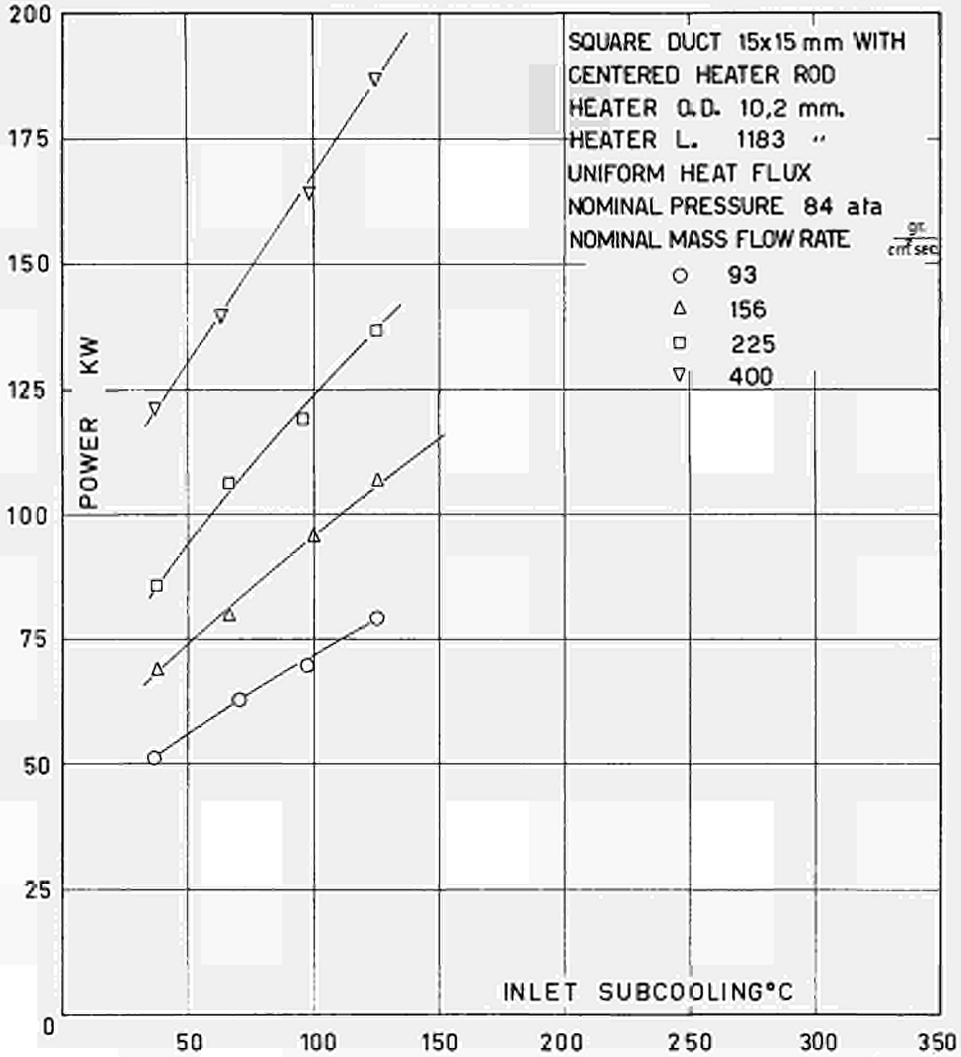

Fig. 8 - Effect of mass flow rate on burnout power. Nominal pressure: 84 ata.

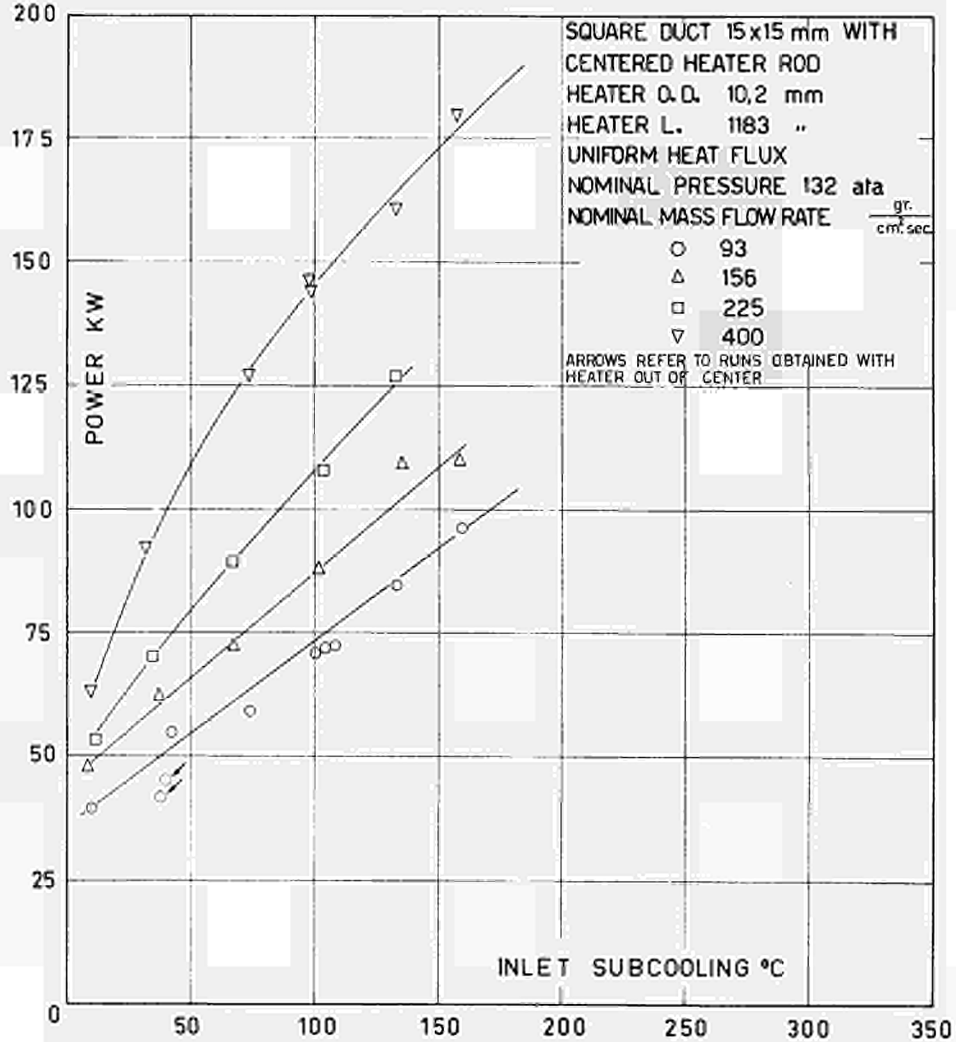

Fig. 9 - Effect of mass flow rate on burnout power. Nominal pressure: 132 ata.

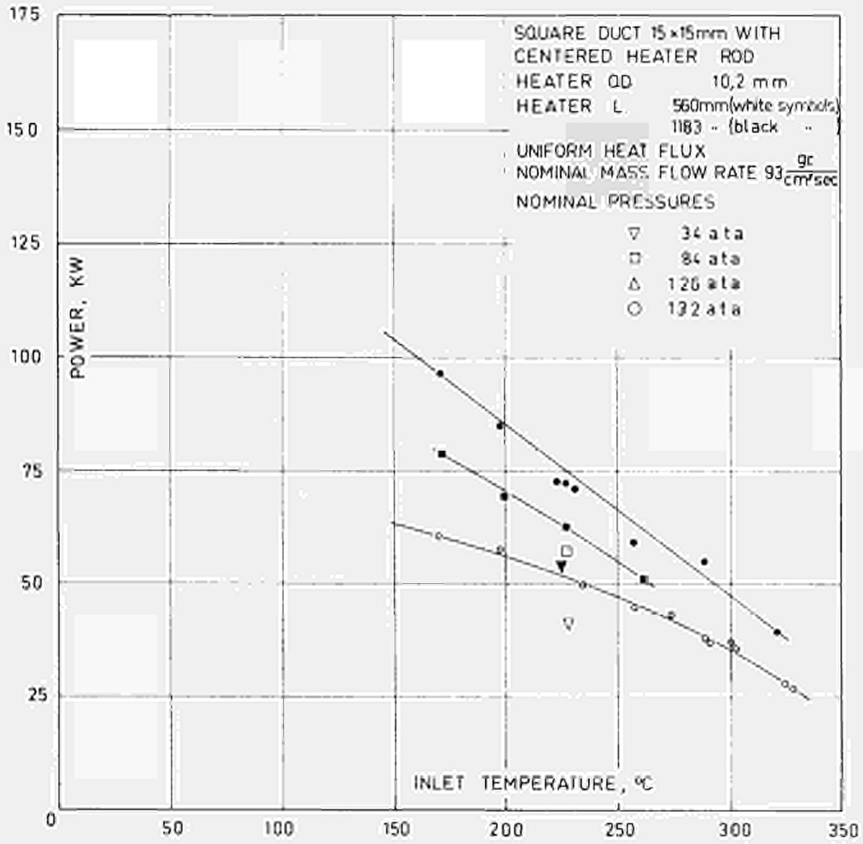

Fig. 10 - Effect of pressure on burnout power. Nominal mass flow rate: 93 $\frac{gr}{cm^2 \cdot sec}$.

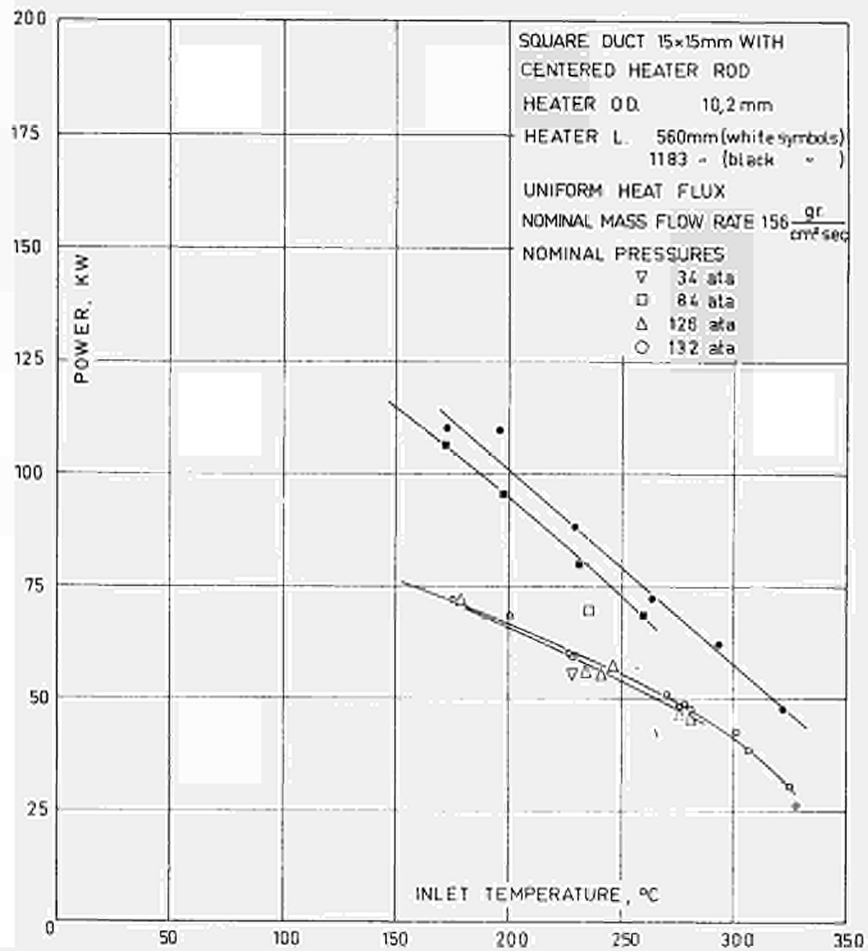

Fig. 11 - Effect of pressure on burnout power. Nominal mass flow rate: 156 $\frac{gr}{cm^2 \cdot sec}$.

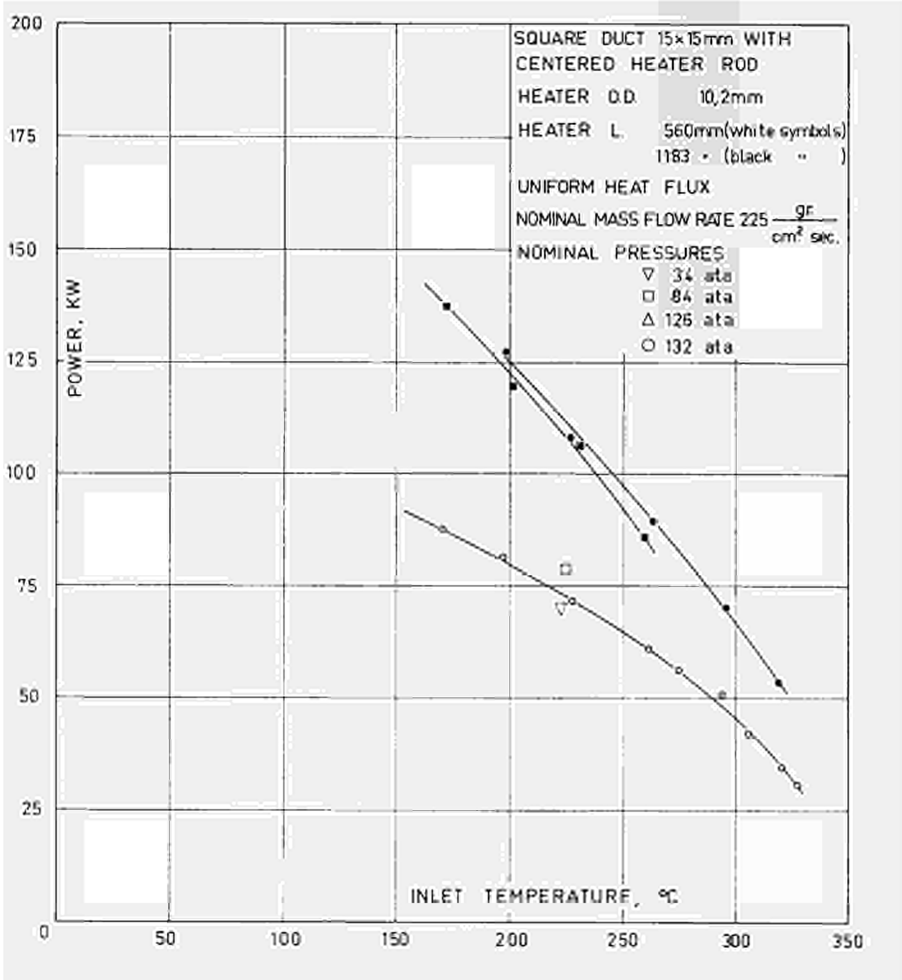

Fig. 12 - Effect of pressure on burnout power. Nominal mass flow rate: 225 $\frac{gr}{cm^2 \cdot sec}$.

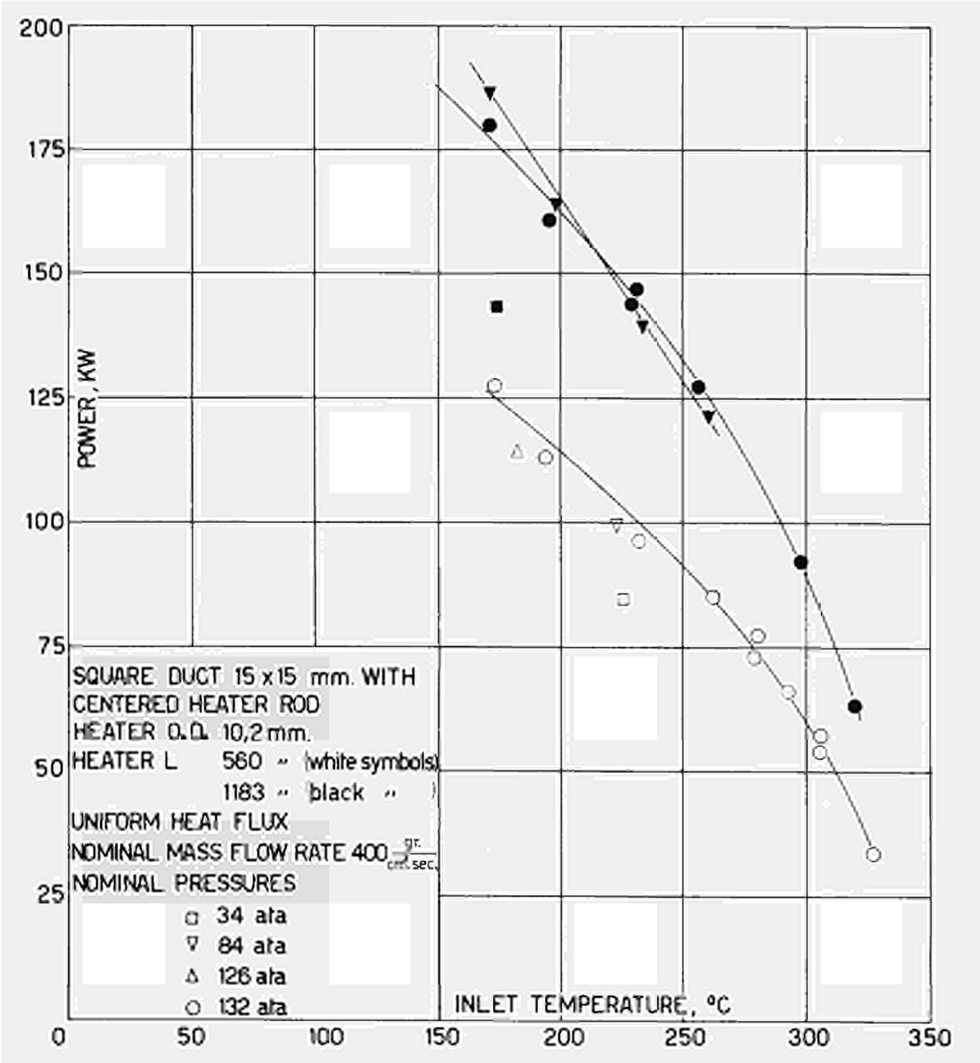

Fig. 13 - Effect of pressure on burnout power. Nominal mass flow rate: 400 $\frac{gr}{cm^2 \cdot sec}$.

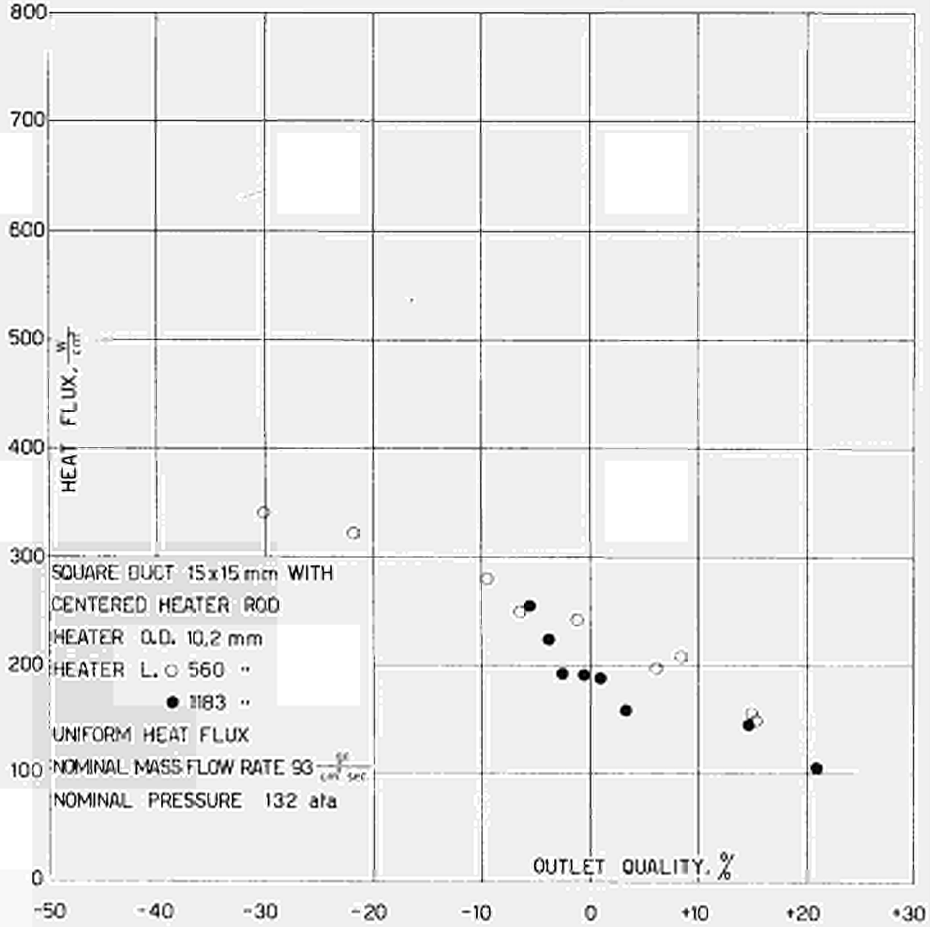

Fig. 14 - Effect of heater length on burnout heat flux. Nominal mass flow rate: 93 $\frac{gr}{cm^2\ sec}$.

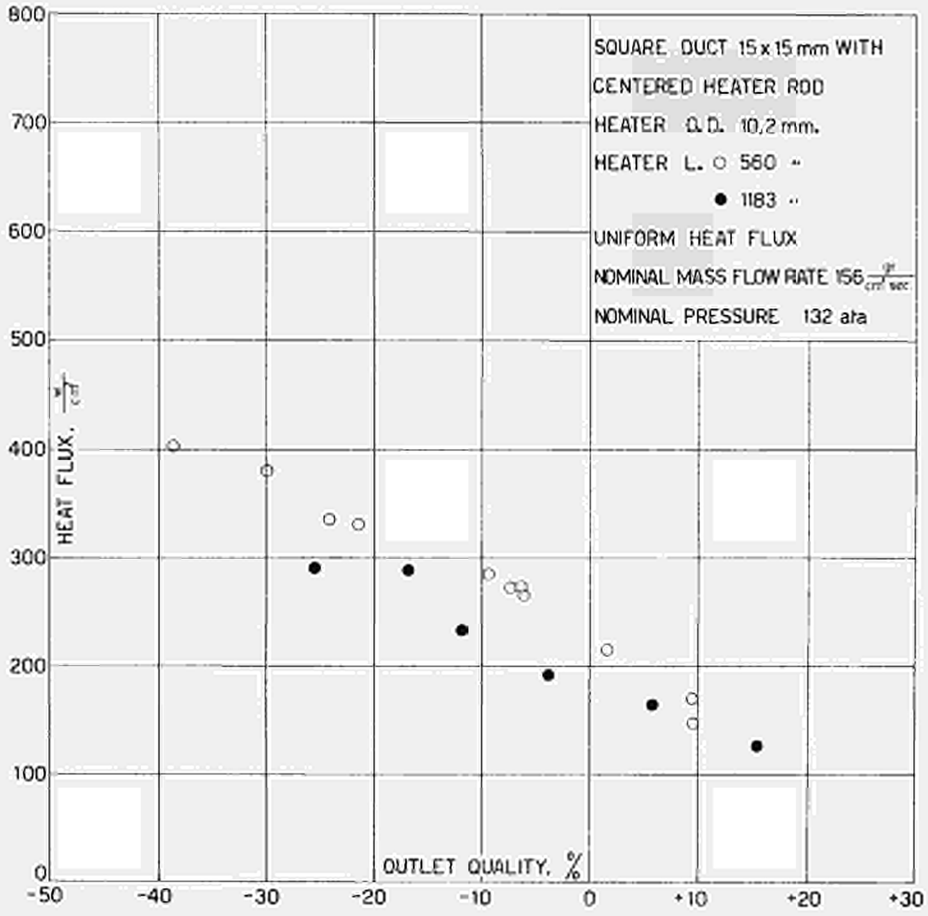

Fig. 15 - Effect of heater length on burnout heat flux. Nominal mass flow rate: 156 $\frac{gr}{cm^2 \cdot sec}$.

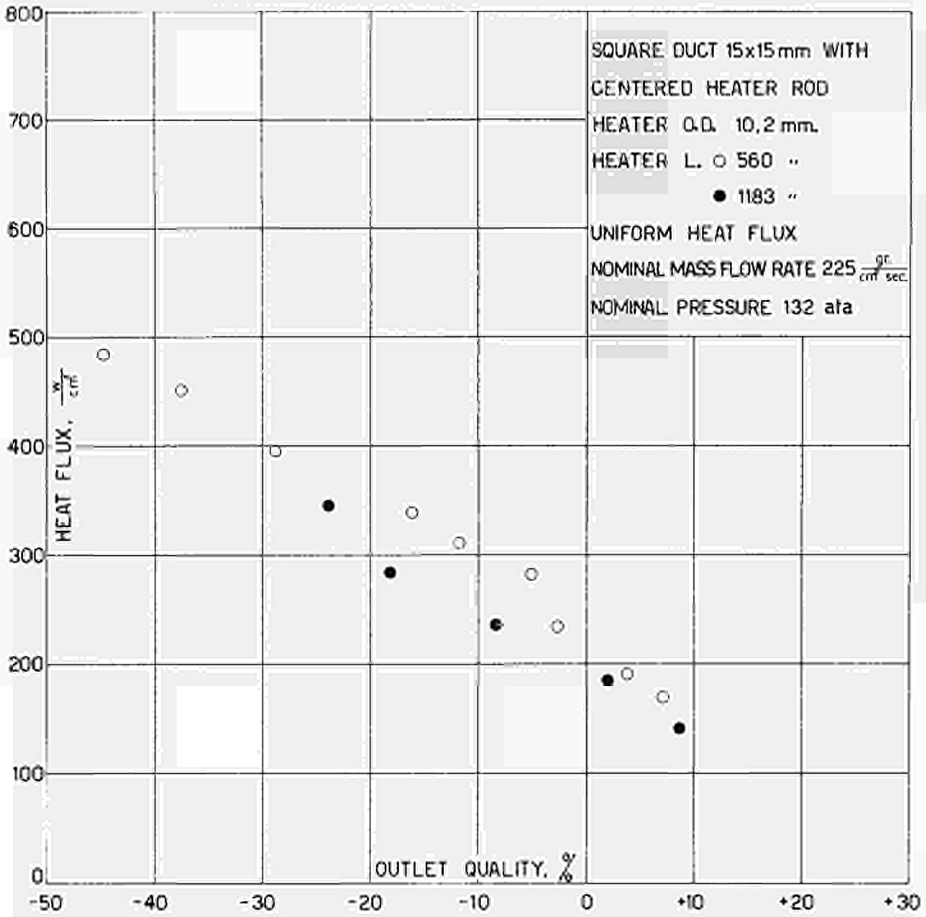

Fig. 16 - Effect of heater length on burnout heat flux. Nominal mass flow rate: 225 $\frac{gr}{cm^2 \cdot sec}$.

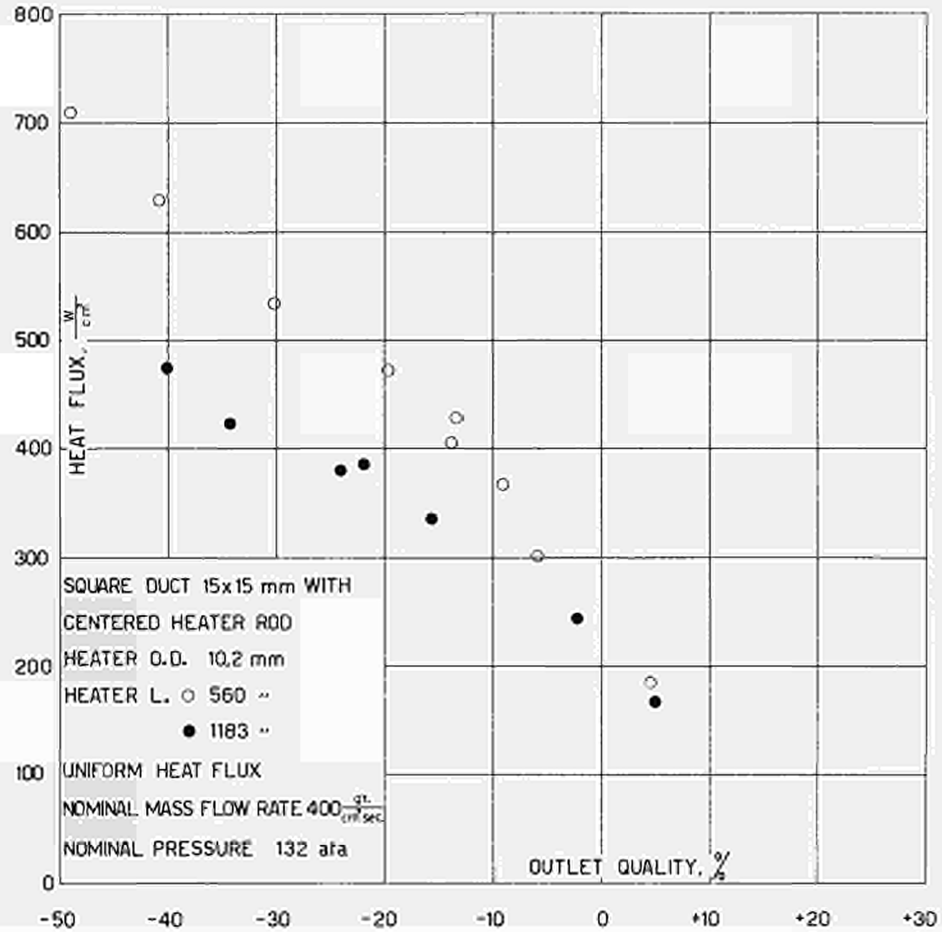

Fig. 17 - Effect of heater length on burnout heat flux. Nominal mass flow rate: 40 $\frac{gr}{cm^2 \cdot sec}$.

NOTICE TO THE READER

All Euratom reports are announced, as and when they are issued, in the monthly periodical **EURATOM INFORMATION**, edited by the Centre for Information and Documentation (CID). For subscription (1 year : US$ 15, £ 5.7) or free specimen copies please write to :

Handelsblatt GmbH
"Euratom Information"
Postfach 1102
D-4 Düsseldorf (Germany)

or

Office de vente des publications
des Communautés européennes
2, Place de Metz
Luxembourg

To disseminate knowledge is to disseminate prosperity — I mean general prosperity and not individual riches — and with prosperity disappears the greater part of the evil which is our heritage from darker times.

Alfred Nobel

SALES OFFICES

All Euratom reports are on sale at the offices listed below, at the prices given on the back of the front cover (when ordering, specify clearly the EUR number and the title of the report, which are shown on the front cover).

PRESSES ACADEMIQUES EUROPEENNES
98, Chaussée de Charleroi, Bruxelles 6

Banque de la Société Générale - Bruxelles
compte N° 964.558,
Banque Belgo Congolaise - Bruxelles
compte N° 2444.141,
Compte chèque postal - Bruxelles - N° 167.37,
Belgian American Bank and Trust Company - New York
compte No. 22.186,
Lloyds Bank (Europe) Ltd. - 10 Moorgate, London E.C.2,
Postscheckkonto - Köln - Nr. 160.861.

OFFICE CENTRAL DE VENTE DES PUBLICATIONS DES COMMUNAUTES EUROPEENNES
2, place de Metz, Luxembourg (Compte chèque postal N° 191-90)

BELGIQUE — BELGIË
MONITEUR BELGE
40-42, rue de Louvain - Bruxelles
BELGISCH STAATSBLAD
Leuvenseweg 40-42 - Brussel

DEUTSCHLAND
BUNDESANZEIGER
Postfach - Köln 1

FRANCE
SERVICE DE VENTE EN FRANCE DES PUBLICATIONS DES COMMUNAUTES EUROPEENNES
26, rue Desaix - Paris 15°

ITALIA
LIBRERIA DELLO STATO
Piazza G. Verdi, 10 - Roma

LUXEMBOURG
OFFICE CENTRAL DE VENTE DES PUBLICATIONS DES COMMUNAUTES EUROPEENNES
9, rue Goethe - Luxembourg

NEDERLAND
STAATSDRUKKERIJ
Christoffel Plantijnstraat - Den Haag

UNITED KINGDOM
H. M. STATIONERY OFFICE
P. O. Box 569 - London S.E.1

EURATOM — C.I.D.
51-53, rue Belliard
Bruxelles (Belgique)